

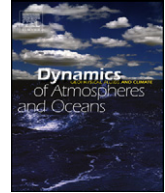


ELSEVIER

Contents lists available at ScienceDirect

Dynamics of Atmospheres and Oceans

journal homepage: www.elsevier.com/locate/dynatmoce



Transport weighted temperature and internal energy transport of the Indonesian throughflow

D. Tillinger*, A.L. Gordon

Lamont-Doherty Earth Observatory of Columbia University, 61 Route 9W, Palisades, NY 10964, United States

ARTICLE INFO

Article history:

Available online 2 February 2010

Keywords:

Indonesian throughflow
El Niño–Southern Oscillation
Makassar Strait
Internal energy transport
Transport weighted temperature
Heat transport

ABSTRACT

A 50-year record of the Indonesian throughflow (ITF) was obtained using the Simple Ocean Data Assimilation (SODA) dataset to calculate a timeseries of Pacific-to-Indian Ocean pressure differences, which were calibrated to transport profiles using ARLINDO (1997) and INSTANT (2004–2006) observational data. The 50 year SODA based ITF transport average is 10.4 Sv; the transport weighted temperature (TWT) is 14.6 °C and the internal energy transport (IET) is 0.53 PW. The different configurations of the ITF transport and temperature profiles result in a dissimilarity in the variability of the IET and the TWT, with the IET more closely correlated with both the depth of the 18 °C isotherm in the western equatorial Pacific and the NINO3.4 index. As with the transport, the IET increases during La Niña and decreases during El Niño. The TWT is only weakly correlated with NINO3.4, suggesting that the El Niño–Southern Oscillation signal is transmitted from the Pacific to the Indian Ocean via changes in pressure and thus in transport rather than by changes in temperature.

© 2010 Elsevier B.V. All rights reserved.

1. Introduction

The Indonesian throughflow (ITF) transfers approximately 10–15 Sv of equatorial Pacific water to the Indian Ocean (Gordon et al., *in press*). Model experiments have shown that the ITF affects the circulation and temperature characteristics of both the Pacific and the Indian Oceans (Hirst and Godfrey, 1993; Potemra and Schneider, 2007). Song et al. (2007) demonstrate that the closure of

* Corresponding author. Tel.: +1 845 365 8571.

E-mail address: debrat@ldeo.columbia.edu (D. Tillinger).

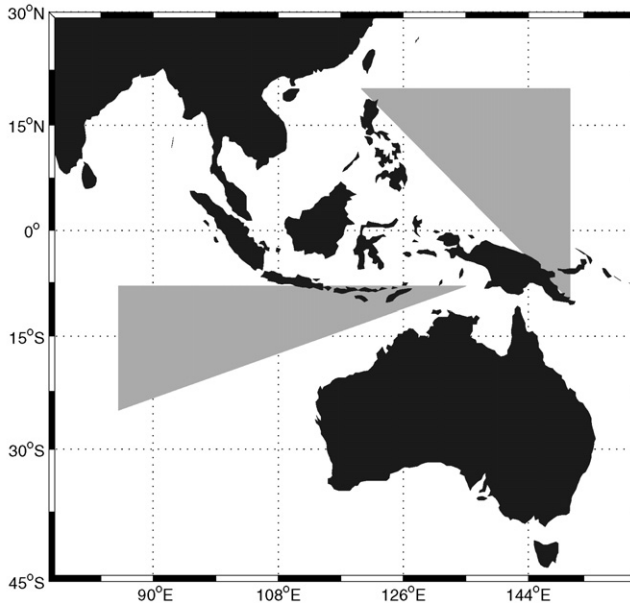


Fig. 1. Map of the Indonesian throughflow region. Shaded areas demarcate the inflow (Pacific) and outflow (Indian) regions of the ITF. Reproduced from Tillinger and Gordon (2009).

the Indonesian interocean pathway shifts the Indo-Pacific warm pool and associated rainfall, and could change the characteristics of El Niño-Southern Oscillation (ENSO) as well. Ffield et al. (2000) showed that the mean temperature of the ITF, particularly within the thermocline, varies with the total transport. Using data from the December 1996 to February 1998 ARLINDO project, they demonstrate that the coupling of the temperature and transport fields act to transmit the ENSO signal from the Pacific Ocean to the Indian Ocean via changes in the internal energy transport (IET).

The objective of our study is to determine the relationship between ITF temperature and transport at interannual and greater timescales. The determination of the ITF transport weighted temperature (TWT) and the IET allows for a distinction between the effects of ENSO-related temperature changes from ENSO-related pressure and transport changes.

2. Data and methodology

The current study requires a long-term timeseries of ITF transport and temperature. Since direct observational timeseries of the ITF are too short, a 50-year record of ITF transport was constructed using Pacific to Indian Ocean pressure gradients from the SODA retrospective analysis model version 2.0.2-4. SODA assimilates observations into a global circulation model (Carton et al., 2000a,b). Monthly data are available from 1958 through 2000 using ECMWF ERA-40 winds and from 2001 to 2007 using QuikSCAT 2 winds. SODA contains 40 vertical levels and a horizontal resolution of 28 km by 44 km on the equator, reducing in resolution poleward. Horizontal friction and diffusion are held constant at $6 \times 10^7 \text{ cm s}^{-2}$, and vertical friction and diffusion are dependent on the Richardson number, with a maximum value of 3 cm s^{-2} .

SODA temperature and salinity data were averaged and used to calculate a monthly timeseries of density and pressure profiles within both the inflow (western Pacific Ocean) and outflow (eastern Indian Ocean) regions of the ITF (Fig. 1). Pressure was interpolated on to regular density intervals. On each of these isopycnals, the spatially averaged pressure from the outflow region was subtracted from the spatially averaged pressure in the inflow region. The depth of these isopycnals within the Makassar Strait was assumed to be the same as their depth in the inflow area, as most of the mixing of the ITF

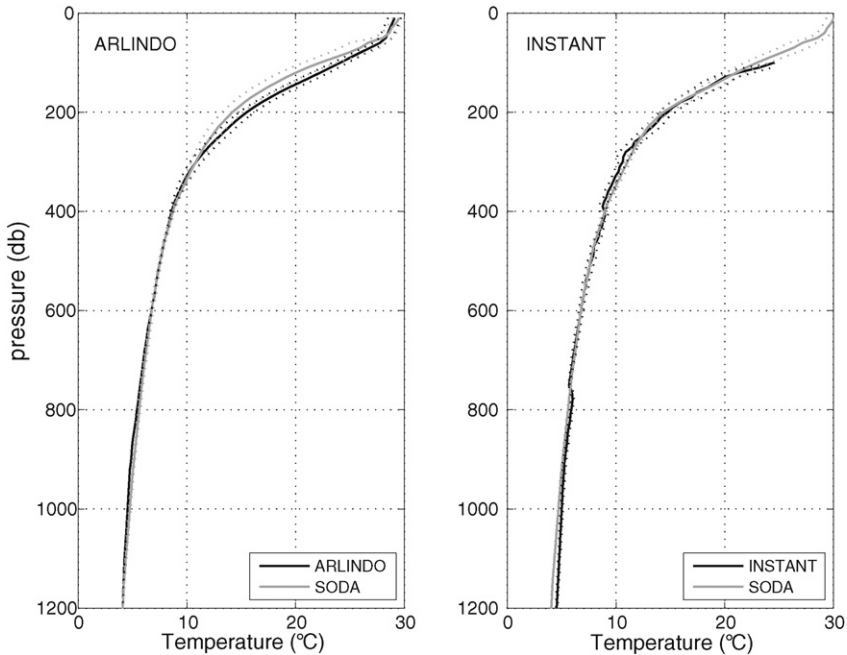


Fig. 2. The average profiles of temperature during the ARLINDO and INSTANT observational periods showing the in situ data (black line) and SODA data (grey line), with one standard deviation from the mean (dotted line).

occurs further downstream in the Banda Sea. These values are defined as positive when the Pacific Ocean pressure exceeds the Indian Ocean pressure. The mean pressure difference was subtracted from the dataset, yielding a timeseries of monthly interocean pressure difference anomalies at 10 db intervals from 10 db below the surface to the effective sill depth of 1200 db (see Tillinger and Gordon, 2009 for a full discussion of this method).

On timescales greater than nine months, the method of using pressure differences on isopycnal layers to calculate ITF transport accurately reproduced the variability of in situ transport data in the Makassar Strait during the 1997–1998 ARLINDO ($r = 0.98$) and 2004–2006 INSTANT ($r = 0.74$) observational periods. Most of the error in the pressure difference timeseries was concentrated in the surface mixed layer.

Pressure differences on isopycnals between the Pacific and Indian Oceans can provide transport variability but not an amount of transport. The ARLINDO (Gordon et al., 1999; Susanto and Gordon, 2005) and INSTANT (Gordon et al., in press; Sprintall et al., 2004) observationally based studies in Makassar Strait were therefore used to calibrate the pressure difference values to transport values. Both studies deployed moorings in the Labani Channel, a 45 km constriction of the Makassar Strait, near 3°S and 118°E. The moorings contained acoustic Doppler current profilers, current meters, and temperature sensors. ARLINDO gathered data for 20 months between December 1996 and July 1998 and INSTANT gathered data from 35 months between January 2004 and November 2006. The data were converted to monthly averages and gridded in 10 db bins. The pressure differences were then calibrated to minimize the error in both observational periods, weighting all months equally.

SODA temperature data used are from within the Labani Channel. They closely approximate in situ data: they are warmer than the vertically averaged in situ temperatures during ARLINDO by an average of 0.04 °C and cooler than INSTANT values by an average of 0.03 °C (Fig. 2). In situ temperature data for the top 100 m of the water column were not available for the INSTANT period. The final transport and temperature values were filtered to remove the annual and semiannual harmonics, so as to isolate interannual signals. The Makassar Strait transport can be considered representative of the

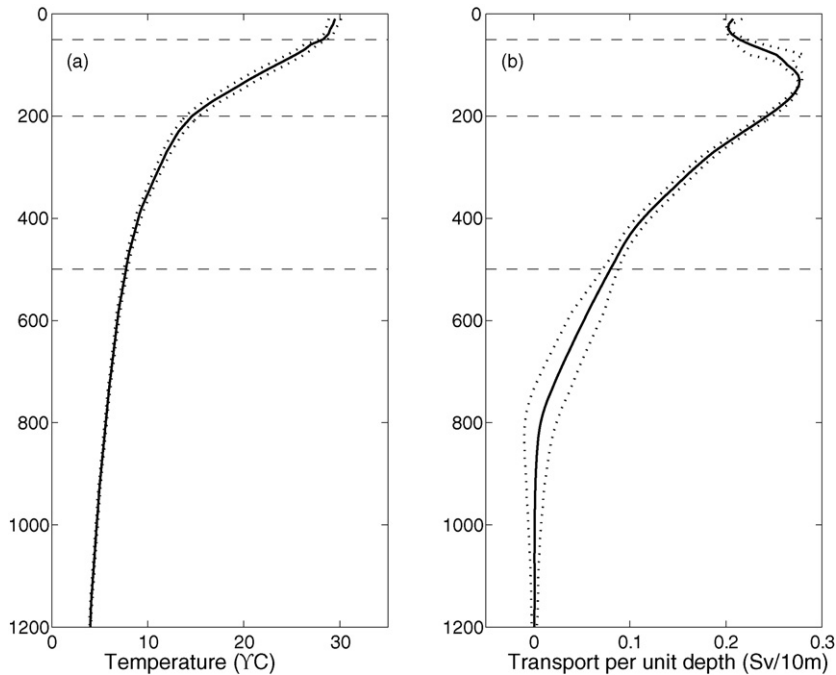


Fig. 3. The average profiles of temperature (panel a, solid line) and transport (panel b, solid line) with one standard deviation from the mean (dotted line), calculated over the 50-year reanalysis period.

thermocline transport of the ITF, with approximately 80% of the total ITF funneled through the Strait (Gordon, 2005; Gordon and Fine, 1996), with the remainder of the flow, through Lifamatola passage, primarily composed of cooler, deeper water (van Aken et al., 2009).

3. Temperature and velocity profiles and variability

The average temperature profile of the ITF within the Makassar Strait (Fig. 3a) is divided into four distinct layers. The well-mixed surface layer (SL, 0–50 m) has a mean vertical temperature gradient of $-0.31\text{ }^{\circ}\text{C}/10\text{ m}$. The thermocline layer (TL, 50–200 m) is characterized by a larger temperature gradient of $-0.91\text{ }^{\circ}\text{C}/10\text{ m}$, which decreases in the middle layer (ML, 200–500 m) to only $-0.23\text{ }^{\circ}\text{C}/10\text{ m}$ and tapers off to $-0.05\text{ }^{\circ}\text{C}/10\text{ m}$ in the deep layer (DL, 500–1200 m).

The profile of average Makassar ITF transport per unit depth (Sv/10 m) within the Makassar Strait (Fig. 3b) differs significantly from the temperature profile. The SL shows very little vertical variability, but the TL shows a distinct transport maximum at 140 m. The transport decreases steadily in the ML, dropping to 0 Sv/10 m within the DL, at approximately 800 m, below the Makassar Strait sill depth of 680 m (Gordon et al., 2003).

The total SODA based 50-year Makassar ITF transport varies from 7.4 Sv to 12.5 Sv, with an average of 10.4 Sv. Transport variability is not distributed equally with depth, but rather is linked to changes in the shape of the transport profile. We find that increased Makassar ITF transport is primarily accomplished within the ML and DL. Although the TL contains the highest velocity, the much thicker ML actually transports slightly more water: 3.9 Sv in the TL and 4.3 Sv in the ML, a difference of 0.4 Sv. To ensure that this difference is not just a result of the SODA derived interocean pressure difference, the calculation was carried out for the ARLINDO and INSTANT datasets. In both observational datasets, the same result was found: the ML transported 0.3 Sv more than the TL during INSTANT and 0.9 Sv more than the TL during ARLINDO.

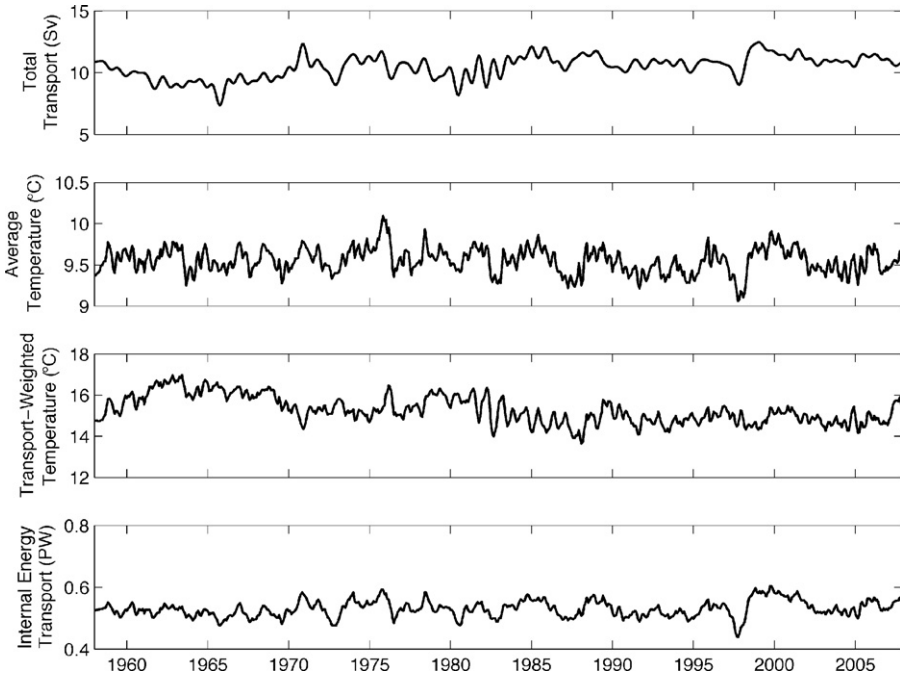


Fig. 4. Timeseries of total transport (panel a), average temperature (panel b), transport weighted temperature (panel c), and internal energy transport (panel d).

4. Transport-weighted temperature

The temporal relationship between the temperature and transport profiles can be captured by the transport-weighted temperature (TWT). The TWT is therefore the average temperature of the water column, weighted by the transport:

$$\text{TWT} = \frac{\int QTdz}{\int Qdz} \quad (1)$$

where Q is the transport in Sv and T is the temperature in °C, evaluated from the sea surface to 1200 m, the effective sill depth (Andersson and Stigebrandt, 2005). Q and T are defined for each of the 10 db layers from the 10 db to 1200 db. Since the concept of TWT is only valid for unidirectional flow, negative transport values, which occur in 15% of the data, are set to zero to produce physically meaningful results. Unlike a simple average of temperature, the TWT is the most representative temperature for the whole water column, as the temperature is weighted most heavily at the location of the transport maximum. Changes in the total transport do not directly influence the TWT calculation, but changes in the profile of transport do.

When TWT is compared with the simple average of temperature and the total transport (Fig. 4), it tracks transport ($r = -0.77$) more closely than it tracks average temperature ($r = 0.34$). As a result of the differences between the temperature and transport profiles as described above, total transport accounts for 60% of the variance in TWT, while average temperature only accounts for 12% of that variance. Since increases in total transport are primarily seen in the lower layers, the TWT will be influenced to a greater degree by cooler water during periods of high transport.

Vranes et al. (2002) calculated TWT for the ARLINDO observational period (December 1996–July 1998). Since the shallowest current meter was located at 200 db, several different extrapolation techniques were used to create a complete profile of velocity to the sea surface. Temperature was calculated from 12 moored temperature sensors and extrapolated to the surface using NCEP sea surface temper-

atures. That study found a Makassar Strait TWT of 14.7 °C to 16.3 °C. Gordon et al. (2008), using the Makassar Strait INSTANT timeseries, finds a TWT of 15.6 ± 3.7 °C. Using interocean pressure gradients from SODA calibrated with the full Makassar observational dataset and temperatures from SODA, we find an average TWT value of 14.6 °C for the 50 year timeseries period. We find a TWT of 14.9 °C for ARLINDO, and 14.7 °C for INSTANT. These values are within the ranges calculated from the in situ data.

Sprintall et al. (2009) examine TWT from INSTANT at the three outflow passages and finds a value of 21.5 °C at Lombok, 17.8 °C at Timor, and 15.2 °C at Ombai. The average of all three passages yields a TWT of 17.9 °C. The transport profiles of these passages differ significantly from that of the Makassar; Lombok and Timor are surface intensified with weaker subsurface maxima at 50–60 m, while Ombai displays equally strong maxima at both the surface and the thermocline. A warmer TWT is therefore expected in the outflow passages as compared to the Makassar, where the transport per unit depth is thermocline intensified. This suggests an input of warmer water to the ITF and/or air to sea heat flux between the Makassar inflow and Sunda passages outflow (Gordon et al., in press).

5. Internal energy transport

The IET across an oceanic section can be approximated as:

$$E = c_p \int \rho v (\theta - \theta_r) d\sigma \quad (2)$$

where c_p is the specific heat per unit mass at constant pressure, ρ is the in situ density, v is the velocity normal to the section, θ is the in-situ potential temperature, θ_r is a reference temperature, and σ is the corresponding area element (Warren, 1999). As with the calculation of TWT, v , θ , and σ are defined based on 10 db layers which are assumed to contain uniform flow and temperature.

If the total Makassar ITF transport were constant in time and a reference temperature of 0 °C were used, the TWT and the IET would differ in units but not in variability. The TWT would then be considered as the IET per unit transport. Although the TWT shows the effect of changes in the transport profile, it is not directly affected by changes in total transport. It is only affected indirectly, since the transport profile and the total transport are not independent. Ultimately, it is the IET that is included in the calculation of a global energy budget.

The reference temperature used in the calculation of the IET is the temperature of the waters of the ITF when they leave the Indian Ocean or when they enter the Pacific Ocean, providing a section of ocean transport and temperature that can be added to the ITF to ensure a closed system with no net mass transport. The value of the reference temperature therefore depends on how the section is closed. Schneider and Barnett (1997) use the average temperature between Australia and Antarctica, which they calculate to be 3.4 °C, as the reference temperature. Schiller et al. (1998) note that the choice is arbitrary and choose to close the section with the flow between Tasmania and 50°S, which has an average temperature of 3.72 °C in their model. Gordon and McClean (1999) follow Schneider and Barnett and use the average temperature between Australia and Antarctica, but they calculate it as 2.8 °C. Ffield et al. (2000) follow Schiller et al. and use 3.72 °C (and also use 0 °C) and Vranes et al. (2002) follow Schneider and Barnett and use 3.4 °C. Estimates from SODA suggest a slightly higher value of 3.7 °C for the section between Australia and Antarctica. Furthermore, that value varies in time from 2.3 °C to 4.5 °C.

Changing the reference temperature changes both the mean value of the IET and its variability. Increasing the temperature from 2.8 °C to 3.7 °C, the range of values used in the aforementioned studies, decreases the average IET by 7.5% and the standard deviation by 8.8%. However, the value of IET calculated with a constant reference temperature varies by 27% over the course of the timeseries. For the sake of comparison to previous studies (Table 1), the reference temperature is adjusted accordingly. Based on the various reference temperatures, the internal energy flux varies from 0.52 PW to 0.68 PW and is closest to the upper limit value of Vranes 2002. For the purposes of examining the variability of the IET, a reference temperature of 3.4 °C is used. Based on that calculation, the 50 year SODA based IET ranges from 0.44 PW to 0.60 PW, with a mean of 0.53 PW.

Table 1

Internal energy and transport values.

Study	Average IE (reference temperature)	Total transport	Average IE in current study (10.5 Sv)
Schneider and Barnett (1997)	0.90 PW (3.4 °C)	13.8 Sv	0.53
Schiller et al. (1998)	1.15 PW (3.7 °C)	16.3 Sv	0.52
Gordon and McClean (1999)	0.66 PW (2.8 °C)	3.9 Sv	0.56
Ffield et al. (2000)	0.39 PW (3.72 °C)	9.3 Sv ^a	0.68
Vranes et al. (2002) (upper limit)	0.57 PW (3.4 °C)	10.3 Sv	0.53
Vranes et al. (2002) (lower limit)	0.24 PW (3.4 °C)	6.9 Sv	0.53

^a Ffield et al., 2000 do not provide an average value for the ITF, but cite Gordon et al., 1999, who provide this value.

Total IET (Fig. 5, bottom panel) strongly co-varies with temperature ($r=0.81$) and transport ($r=0.70$), but not with TWT ($r=-0.7$). Since the reference temperature used is cooler than any temperature within the water column of the Makassar ITF, IET is always positive in the direction of mass transport. Negative velocities, which were set to zero in the TWT calculation, act to decrease the net IET. Given that the IET is calculated here with the cooler waters of the Makassar Strait and not the warmer waters of the Sunda passages, it is an estimate of the internal energy exported from the Pacific Ocean, not that which is imported to the Indian Ocean.

6. The relationship of temperature and transport variability to ENSO

The NINO3.4 index is a strong predictor of IET, with increased (decreased) IET during a La Niña (El Niño) event (Fig. 6). It is only weakly correlated with TWT, showing slightly warmer (cooler) temperatures during a La Niña (El Niño) event. During an El Niño event, the 18 °C isotherm within the western Pacific Ocean shoals by an average of 15 m, and thus decreasing the Pacific to Indian pressure gradient and the accompanying transport (Fig. 5). The IET is greatly diminished both because there is less volume transport, and because the water being transported is cooler. TWT, however, varies only slightly with NINO3.4, as the effect of cooler water in the TL is balanced by the increase in relative

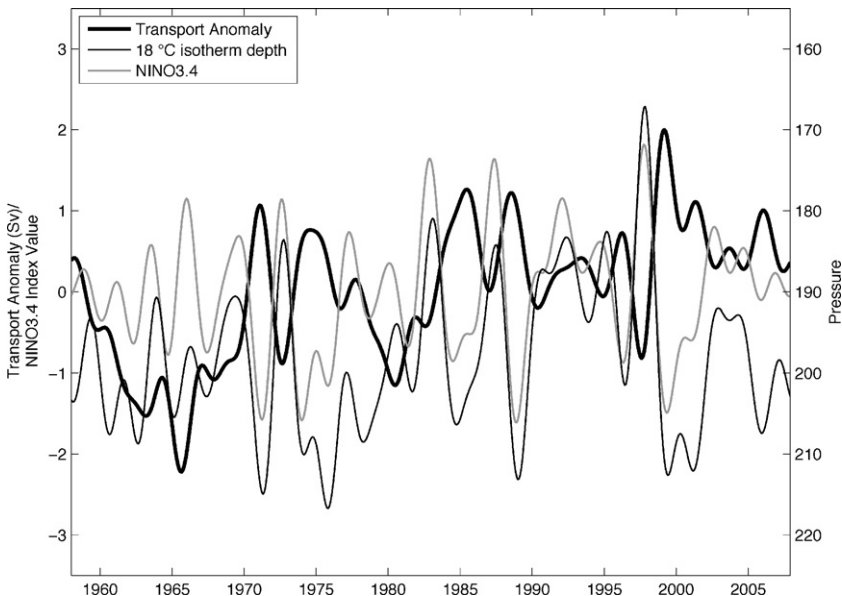


Fig. 5. Timeseries of the IET and NINO3.4 index.

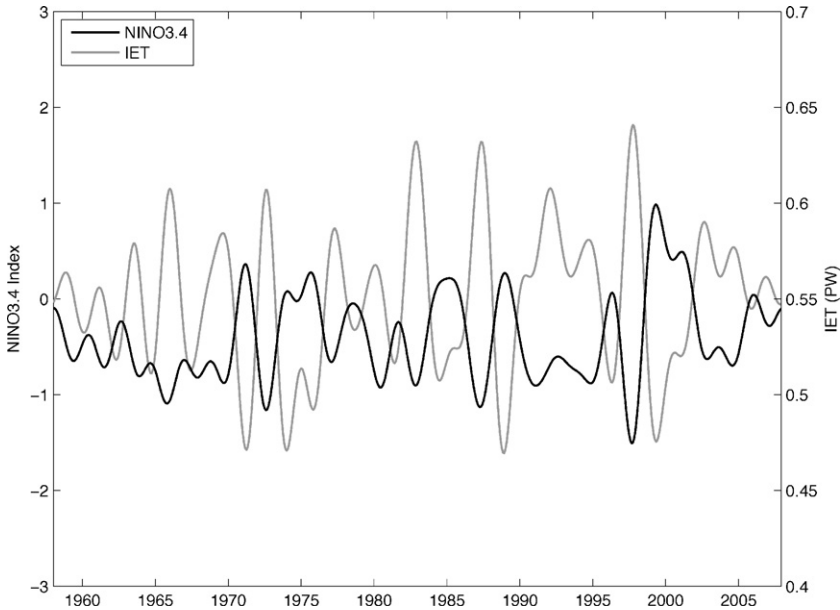


Fig. 6. Timeseries of total transport anomaly (thick black line), the depth of the 18 °C isotherm (thin black line), and the NINO3.4 index (solid grey line), smoothed with 2-year low-pass filter.

transport in that layer. During months with an NINO3.4 value above 1 (i.e. El Niño conditions), the amount of transport within each layer decreases, but the percentage of total transport within the TL increases from 37% to 39%, while the water cools by 0.76 °C. The same effect is seen in the ML, in which relative transport increases from 41% to 42% of the total transport despite a decrease in the amount of transport, and temperature decreases by 0.24 °C. In contrast, the DL transport compensates for the relative increases in the upper layers with a decrease from 11% of the total to 9% of the total and an even greater decrease in the amount of transport, but cools by only 0.04 °C. The opposite effect is seen when NINO3.4 is less than -1 (La Niña): the TL decreases to 35% of the transport and warms by 0.71 °C, the ML decreases to 39% of the transport and warms by 0.16 °C, and the DL increases to 16% of the transport and warms by 0.06 °C.

Therefore, during an El Niño event the effect of cooler water in the TL and ML, which would otherwise act to decrease the TWT, is compensated for by the increase in relative transport in those layers (noting that their waters are still warmer than those of the underlying DL). In contrast, the internal energy decreases simply because both the transport and the temperature of the water within each layer have decreased. The ENSO signal of the Pacific Ocean is therefore transmitted to the Indian Ocean not by the change in TWT but by the accompanying change in pressure that leads to a change in total transport.

7. Conclusions

The thermocline intensification of the ITF transport profile within Makassar Strait results in a disconnect between the TWT and the IET. Given the use of a reference temperature below the in situ temperature, as we see here, IET will always increase as total transport increases. It will, however, show a greater increase when the transport increases at warmer layers rather than cooler ones. In contrast, the TWT will only increase if there is a relative increase in transport in a warm layer. Thus, an increase in transport in the ML or DL, if everything else were held constant, would result in a lower TWT and a higher IET. By examining the temperature and transport profiles of the ITF in the Makassar

Strait, we therefore propose that the ENSO signal is transferred from the Pacific to the Indian Ocean not by changes in temperature but primarily by changes in transport.

Acknowledgements

This research was funded by NSF grant OCE 07-25935. We thank Hsien Ou and Xiaojun Yuan for helpful discussions. Lamont-Doherty Earth Observatory contribution number 7338.

References

- Andersson, H.C., Stigebrandt, A., 2005. Regulation of the Indonesian throughflow by baroclinic draining of the North Australian Basin. *Deep-Sea Research* 1 52, 2214–2233.
- Carton, J.A., Chepurin, G., Cao, X., Giese, B.S., 2000a. A Simple Ocean Data Assimilation analysis of the global upper ocean 1950–95. Part 1: methodology. *Journal of Physical Oceanography* 30 (2), 294–309.
- Carton, J.A., Chepurin, G., Cao, X.H., 2000b. A Simple Ocean Data Assimilation analysis of the global upper ocean 1950–95. Part 2: results. *Journal of Physical Oceanography* 30 (2), 311–326.
- Ffield, A., Vranes, K., Gordon, A.L., Susanto, R.D., Garzoli, S.L., 2000. Temperature variability within Makassar Strait. *Geophysical Research Letters* 27 (2), 237–240.
- Gordon, A.L., 2005. Oceanography of the Indonesian Seas and their Throughflow. *Oceanography* 18 (4), 14–27.
- Gordon, A.L., Fine, R.A., 1996. Pathways of water between the Pacific and Indian oceans in the Indonesian Seas. *Nature* 379, 146–149.
- Gordon, A.L., Giulivi, C.F., Ilahude, A.G., 2003. Deep topographic barriers within the Indonesian seas. *Deep-Sea Research* 50 (12–13), 2205–2228.
- Gordon, A.L., McClean, J.L., 1999. Thermohaline stratification of the Indonesian Seas: model and observations. *Journal of Physical Oceanography* 29 (2), 198–216.
- Gordon, A.L., Susanto, R.D., Ffield, A., 1999. Throughflow within the Makassar Strait. *Geophysical Research Letters* 26 (21), 3325–3328.
- Gordon, A.L., et al., 2008. Makassar Strait Throughflow, 2004 to 2006. *Geophysical Research Letters* 35 (24), doi:10.1029/2008GL036372.
- Gordon, A.L., Sprintall, J., Van Aken, H.M., Susanto, D., Wijffels, S., Molcard, R., Ffield, A., Pranowo, W., Wirasantosa, S. The Indonesian Throughflow during 2004–2006 as observed by the INSTANT program. *Dynamics of Atmosphere and Ocean: “Modeling and Observing the Indonesian Throughflow”*. In: Gordon, A.L., Kamenkovich, V.M. (Guest Editors), doi:10.1016/j.dynatmoce.2009.12.002, in press.
- Hirst, A.C., Godfrey, J.S., 1993. The role of Indonesian throughflow in a global ocean gcm. *Journal of Physical Oceanography* 23 (6), 1057–1086.
- Potemra, J.T., Schneider, N., 2007. Interannual variations of the Indonesian throughflow. *Journal of Geophysical Research* 112, doi:10.1029/2006JC003808.
- Schiller, A., Godfrey, J.S., McIntosh, P.C., Meyers, G., Wijffels, S.E., 1998. Seasonal near-surface dynamics and thermodynamics of the Indian Ocean and Indonesian throughflow in a global ocean general circulation model. *Journal of Physical Oceanography* 28 (11), 2288–2312.
- Schneider, N., Barnett, T.P., 1997. Indonesian throughflow in a coupled general circulation model. *Journal of Geophysical Research-Oceans* 102 (C6), 12341–12358.
- Song, Q., Vecchi, G.A., Rosati, A.J., 2007. Indian Ocean variability in the GFDL coupled climate model. *Journal of Climate* 20 (13), 2895–2916.
- Sprintall, J., et al., 2004. INSTANT: a new international array to measure the Indonesian throughflow. *Eos* 85 (39).
- Sprintall, J., Wijffels, S., Molcard, R., Jaya, I., 2009. Direct estimates of the Indonesian throughflow entering the Indian Ocean: 2004–2006. *Journal of Geophysical Research*, 114, doi:10.1029/2008JC005257.
- Susanto, R.D., Gordon, A.L., 2005. Velocity and transport of the Makassar Strait throughflow. *Journal of Geophysical Research* 110 (C1), doi:10.1029/2004JC002425.
- Tillinger, D., Gordon, A.L., 2009. Fifty years of the Indonesian Throughflow. *Journal of Climate* 22, 6342–6355.
- van Aken, H.M., Brodjonegoro, I.S., Jaya, I., 2009. The deep-water motion through the Lifamatola Passage and its contribution to the Indonesian throughflow. *Deep-Sea Research Part I-Oceanographic Research Papers* 56 (8), 1203–1216.
- Vranes, K., Gordon, A.L., Ffield, A., 2002. The heat transport of the Indonesian Throughflow and implications for the Indian Ocean heat budget. *Deep-Sea Research Part II-Topical Studies in Oceanography* 49 (7–8), 1391–1410.
- Warren, B.A., 1999. Approximating the energy transport across oceanic sections. *Journal of Geophysical Research-Oceans* 104 (C4), 7915–7919.